



Highly polarized luminescence from an AIEE-active luminescent liquid crystalline film



Junqing Sha^a, Hongbo Lu^{a, b, *}, Mengyi Zhou^a, Guo Xia^{a, c}, Yong Fang^a,
Guobing Zhang^{a, b}, Longzhen Qiu^{a, b}, Jiaxiang Yang^d, Yunsheng Ding^b

^a Key Lab of Special Display Technology, Ministry of Education, National Engineering Lab of Special Display Technology, State Key Lab of Advanced Display Technology, Academy of Opto-Electronic Technology, Hefei University of Technology, Hefei, 230009, People's Republic of China

^b Key Laboratory of Advanced Functional Materials and Devices, Anhui Province, School of Chemistry and Chemical Engineering, Hefei University of Technology, Hefei, Anhui 230009, People's Republic of China

^c Key Laboratory of Optical Calibration and Characterization, Anhui Institute of Optics and Fine Mechanics, Chinese Academy of Sciences, Hefei, 230031, China

^d College of Chemistry and Chemical Engineering, Anhui University, Hefei, 230601, People's Republic of China

ARTICLE INFO

Article history:

Received 22 May 2017

Received in revised form

27 June 2017

Accepted 29 July 2017

Available online 2 August 2017

Keywords:

Luminescent liquid crystal

Aggregation-induced enhanced emission

In-plane electric field

Polarized luminescence

ABSTRACT

Luminescent liquid crystals (LLCs) have attracted significant interest for organic optoelectronic applications, especially for the generation of linear polarized light. Here, a novel LLC molecule, 2-(4-(non-anealkoxy)phenyl)-3-(4-formamidophenyl)-acrylonitrile (CN-NPFA), is reported, which shows strong fluorescence in the solid state due to the aggregation-induced enhanced emission (AIEE) effect. Moreover, a well-aligned liquid crystalline film using AIEE-active molecules, is obtained using an in-plane electric field with an alignment layer. It exhibits highly polarized luminescence ($\rho = 0.74$) with a high fluorescence quantum yield. The device is both cheap and easy to fabricate, and has the potential to be used in practical electro-optic applications.

© 2017 Elsevier B.V. All rights reserved.

1. Introduction

Polarized luminescence is important because it is useful for many optoelectronic applications, such as optical information storage devices, stereoscopic displays, and liquid crystal displays [1–8]. Emitted light from a single luminescent molecule is usually polarized; however, light emitted from bulk materials is typically unpolarized because its constituent molecules are not aligned [2]. Inducing the luminescent molecules into an ordered array is a key requirement to produce polarized luminescence [1,3,9].

Liquid crystals (LCs) have thermodynamically stable phases between the isotropic liquid state and crystalline solid state. The combination of long-range orientation ordering with relatively free movement of anisotropic molecules endows liquid crystals with

interesting properties, including the ability to self-assemble. Liquid crystals form supramolecular assemblies with unidirectional orientations of the molecular axis in nature to produce optical anisotropy [10–13]. Luminescent liquid crystals (LLCs) are rapidly emerging as an important optical class of materials, which possess the properties of intrinsic light emission and unique supramolecular organization [14–16]. Currently, the design and synthesis of luminescent liquid crystals is still a challenging task [9,17,18]. It is hard to incorporate luminescent functional groups into LCs while retaining their mesomorphic properties [19,20]. Linear π -conjugated organic luminophores usually show strong luminescence in diluted solutions; however, their luminescence is often reduced or even quenched in the condensed phase because of the aggregation-caused quenching (ACQ) effect [21–23]. Unfortunately, many practical applications require strong luminescence in the aggregated state because the solid state is preferred for better morphological stability.

On the other hand, aggregation-induced enhanced emission (AIEE) has been observed in silole and α -cyanostilbenic derivatives, which is the opposite of ACQ: these luminophores are highly emissive after aggregate formation due to the restriction of

* Corresponding author. Key Lab of Special Display Technology, Ministry of Education, National Engineering Lab of Special Display Technology, State Key Lab of Advanced Display Technology, Academy of Opto-Electronic Technology, Hefei University of Technology, Hefei, 230009, People's Republic of China.

E-mail address: bozhilu@hfut.edu.cn (H. Lu).

intramolecular motion (RIM) [24,25]. Based on the AIEE effect, a variety of new α -cyanostilbenic derivatives have been identified. The luminescent liquid crystals, (2*Z*,-2'*Z*)-2,2'-(1,4-phenylene) bis(3-(4-(dodecyloxy)phenyl) acrylonitrile) – referred to as PDPA, and (Z)-2-(4-Aminophenyl)-3-(4-(dodecyloxy)phenyl) acrylonitrile – referred to as (Z)-CN-APHP, exhibit enhanced fluorescence in the solid states [2,26,27]. The angle between the emission dipole moment and long molecular axis of α -cyanostilbenic LLC produce a lower luminescent dichroic ratio.

In this study, a new α -cyanostilbenic LLC, 2-(4-(nonanealkoxy)phenyl)-3-(4-formamidephenyl)-acrylonitrile (CN-NPFA), was designed and synthesized, which shows a high fluorescent quantum yield in the solid state ($\phi_f = 0.44$). The in-plane electric field induce the uniaxial orientation of the CN-NPFA molecules, in which molecular polar directors are aligned in the direction of the electric field. Upon excitation, the oriented LLC film emits linearly polarized light with high degree of polarization.

2. Experimental section

2.1. Materials and methods

All chemicals were purchased from commercial sources and used without further purification. The synthetic route for 2-(4-(nonanealkoxy)phenyl)-3-(4-formamidephenyl)-acrylonitrile (CN-NPFA) is described in the supporting information (Scheme S1). ^1H NMR (600 MHz) spectra and ^{13}C NMR (150 MHz) spectra were recorded using an Agilent VNMRS600 spectrometer. Infrared (IR) spectra were recorded using a Nicolet 380 Fourier Transform IR (FTIR) spectrometer. Mass spectra were obtained using an Acquity UPLC LCT Premier XE mass spectrometer. Photoluminescence (PL) spectra, fluorescent lifetime and quantum yields were recorded using a Horiba FluoroMax-4 spectrofluorometer. This was done for samples in both solid and solution states. Thermogravimetric analysis (TGA) was conducted with a Netzsch STA449F3 TG at a heating rate of $10\text{ }^\circ\text{C min}^{-1}$. Differential scanning calorimetry (DSC) was performed with a Mettler 821e/400 DSC at a heating and cooling rate of $5\text{ }^\circ\text{C min}^{-1}$. Polarizing optical images and fluorescent images were recorded with an E600POL metallographic microscope (Leica DM2500M) and a 365 nm excitation laser (Coherent). The scanning electron microscope (SEM) images were obtained with a SU8020 SEM. The profile images were recorded using a Zeiss LSM700 confocal microscope and a NanoMap-PS step-height measuring instrument.

2.2. Synthesis of 4-(nonanealkoxy)phenylacetonitrile (T_1)

A mixture of 4-Hydroxyphenylacetonitrile (3.99 g, 0.03 mol) and potassium carbonate (8 g, 0.06 mol) was dissolved in *N,N*-dimethylformamide (40 mL) and stirred at $90\text{ }^\circ\text{C}$ for 15 min. Afterwards, 1-bromononane (6.21 g, 0.03 mol) was added, and the mixture was stirred at $90\text{ }^\circ\text{C}$ for 12 h. The mixture was washed with deionized water and extracted with ethyl acetate three times and dried over MgSO_4 . Finally, after performing silica gel column chromatography, the product was recrystallized to produce a yellow solid (6.72 g) with a yield of 86.5%.

^1H NMR (CDCl_3 , 600 MHz, $\delta = \text{ppm}$): 7.21 (d, 2 H, ArH, $J = 6.0\text{ Hz}$), 6.88 (d, 2 H, ArH, $J = 6.0\text{ Hz}$), 3.94 (t, 2 H, CH_2 , $J = 6.0\text{ Hz}$), 3.67 (s, 2 H, CH_2), 1.77 (m, 2 H, CH_2 , $J = 6.0\text{ Hz}$), 1.30 (m, 12 H, CH_2 , $J = 6.0\text{ Hz}$), 0.88 (t, 3 H, CH_3 , $J = 6.0\text{ Hz}$).

^{13}C NMR (CDCl_3 , 150 MHz, $\delta = \text{ppm}$): 161.54, 131.68, 124.10, 120.93, 117.70, 70.78, 34.53, 32.19, 32.05, 31.92, 31.85, 28.67, 25.50, 25.34, 16.79.

FT-IR (KBr, cm^{-1}): 2918 (s), 2850 (s), 2245 (w), 1602 (m), 1506

(s), 1458 (m), 1391 (m), 1247 (s), 1170 (s), 1110 (m), 1017 (s), 898 (m), 806 (s), 758 (m), 714 (m).

HRMS (MALDI-TOF) m/z : Found: $[\text{M}+\text{H}]^+$ 260.1924; molecular formula $\text{C}_{17}\text{H}_{25}\text{NO}$ requires $[\text{M}+\text{H}]^+$ 260.1936.

2.3. Synthesis of 2-(4-(nonanealkoxy)phenyl)-3-(4-formamidephenyl)-acrylonitrile (CN-NPFA)

A mixture of T_1 (5.18 g, 0.02 mol) and NaOH (0.8 g, 0.02 mol) was dissolved in ethanol and stirred at $78\text{ }^\circ\text{C}$ for 30 min. Then 4-cyanobenzaldehyde (2.62 g, 0.02 mol) was added, and the mixture was stirred at $78\text{ }^\circ\text{C}$ for 3 h. After the solid was filtered off, the crude product was performed silica gel column and recrystallized to give a white powder (5.63 g) with a yield of 72.2%.

^1H NMR (DMSO, 600 MHz, $\delta = \text{ppm}$): 8.05 (s, 1 H, NH), 7.97 (d, 2 H, ArH, $J = 6.0\text{ Hz}$), 7.95 (s, 1 H, CH), 7.92 (d, 2 H, ArH, $J = 6.0\text{ Hz}$), 7.69 (d, 2 H, ArH, $J = 12.0\text{ Hz}$), 7.47 (s, 1 H, NH), 7.05 (d, 2 H, ArH, $J = 12.0\text{ Hz}$), 4.00 (t, 2 H, CH_2 , $J = 6.0\text{ Hz}$), 1.70 (m, 2 H, CH_2 , $J = 6.0\text{ Hz}$), 1.39 (m, 2 H, CH_2 , $J = 6.0\text{ Hz}$), 1.25 (m, 10 H, CH_2 , $J = 6.0\text{ Hz}$), 0.84 (t, 3 H, CH_3 , $J = 6.0\text{ Hz}$).

^{13}C NMR (DMSO, 150 MHz, $\delta = \text{ppm}$): 163.43, 140.86, 139.43, 135.22, 132.00, 130.25, 128.40, 120.97, 119.97, 117.79, 115.67, 70.98, 34.51, 32.16, 32.01, 31.89, 31.78, 28.63, 25.31, 21.08, 16.74.

FT-IR (KBr, cm^{-1}): 3379 (s), 3203 (s), 2920 (s), 2843 (m), 2219 (w), 1655 (s), 1603 (m), 1510 (m), 1422 (s), 1246 (s), 1158 (m), 1022 (vs), 936 (w), 828 (m), 750 (m).

HRMS (MALDI-TOF) m/z : Found: $[\text{M}+\text{H}]^+$ 391.2293; molecular formula $\text{C}_{25}\text{H}_{30}\text{N}_2\text{O}_2$ requires $[\text{M}+\text{H}]^+$ 391.2307.

2.4. Fabrication of a highly polarized fluorescent film

A patterned indium tin oxide (ITO) substrate with a $10\text{ }\mu\text{m}$ wide electrode and a $10\text{ }\mu\text{m}$ wide space was prepared. Polyimide (PI) solution was poured onto the patterned ITO substrate to produce the rubbing alignment layer, see Fig. S1. The original CN-NPFA film was prepared by spin-coating at lower revolving speed with approximately $9\text{ }\mu\text{m}$ height. The highly polarized luminescent film on the substrate was obtained after CN-NPFA cooled down to room temperature from its nematic phase with a cooling rate of $1\text{ }^\circ\text{C min}^{-1}$ and an applied direct-current voltage of 200 V.

3. Results and discussion

CN-NPFA emits blue fluorescent light both in solution and solid states. As shown in Fig. 1(a), CN-NPFA was weakly emissive when dissolved in a good solvent (DMF) showing moderate quantum yields ($\phi_f = 0.17$). The luminescence is distinctly enhanced in its solid-state, which shows high quantum yields ($\phi_f = 0.44$). These results indicate that CN-NPFA is AIEE active. Fig. 1(b) displays the luminescence decay profiles of CN-NPFA solution and powders. According to the calculation results based on density functional theory (DFT), the optimized geometry of CN-NPFA is rod-like and twisted in the isolated state due to internal steric repulsions – see Fig. S2. The relatively higher non-radiative rate-constant ($k_{nr} = (1 - \phi_f)/\tau_F = 2.8 \times 10^9\text{ s}^{-1}$) than radiative rate-constant ($k_r = \phi_f/\tau_F = 2.1 \times 10^8\text{ s}^{-1}$) of CN-NPFA in DMF solution is mainly a consequence of the nonplanarity and torsional relaxation of the CN-NPFA molecule in the isolated state. On the other hand, for the aggregation state, the non-radiative rate-constant ($k_{nr} = 2.4 \times 10^8\text{ s}^{-1}$) is one order of magnitude smaller than that in solution, while the radiative rate-constant ($k_r = 1.9 \times 10^8\text{ s}^{-1}$) is about the same order of magnitude as in solution, which gives the peculiar AIEE effect (see Fig. 2).

To confirm the visual observation, the photoluminescence (PL) spectra of CN-NPFA in DMF solution and DMF/water mixtures were

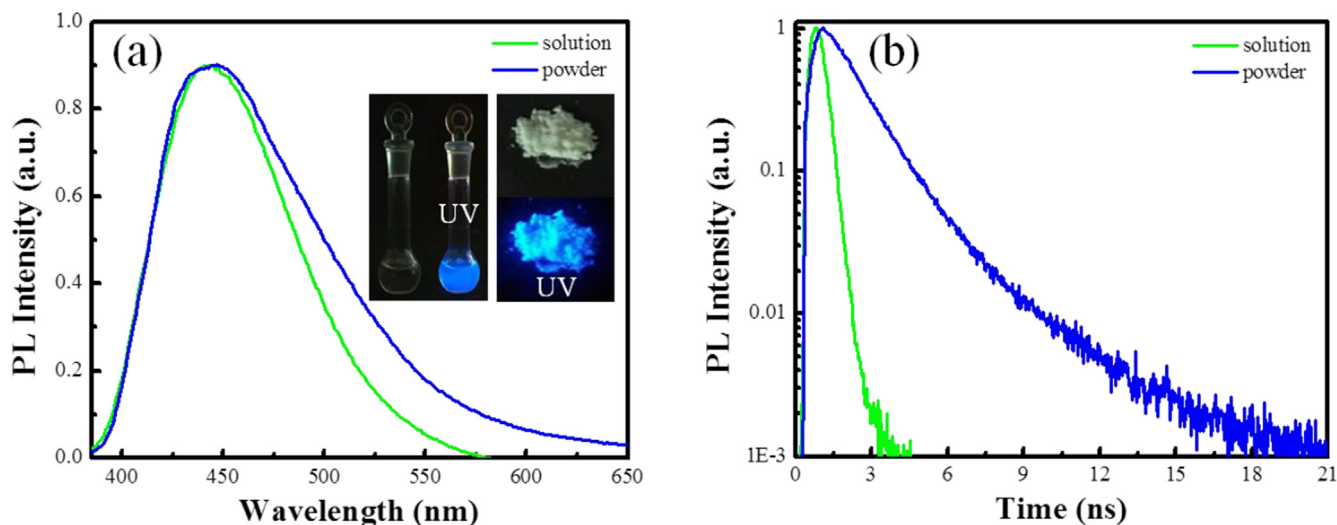


Fig. 1. (a) PL spectra of CN-NPFA solution and powder. Insets are the photo of CN-NPFA in solution and solid state under natural and UV (365 nm) light. (b) The fluorescent lifetime of CN-NPFA in solution and condensed states.

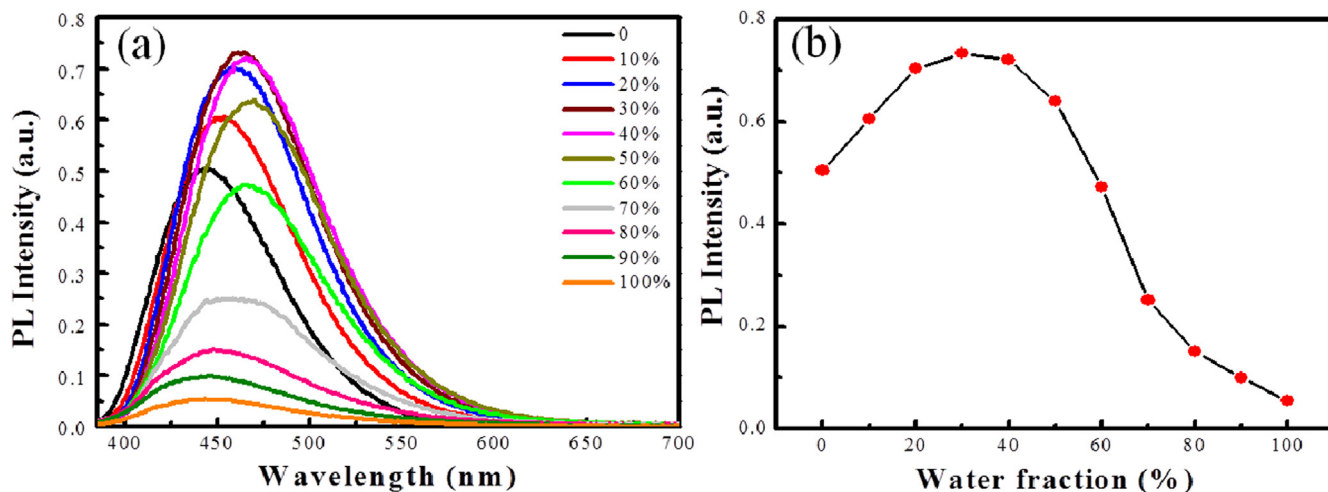


Fig. 2. (a) PL intensity spectra of CN-NPFA in DMF and H₂O/DMF mixtures. (b) PL peak intensity as a function of water content.

investigated. Water was used because it does not dissolve CN-NPFA, hence, the luminescent molecules will aggregate in the aqueous mixtures with high water fractions. With the addition of pure water to the DMF solution, the PL intensity increases accordingly and the PL peak red-shifts slowly to 462 nm from 442 nm. The highest emission was obtained in a DMF/water mixture with 30% water. In a good solvent (DMF), the benzene rings of the CN-NPFA molecule can rotate freely around a single-link, which consumes the energy of the excited state and results in weak fluorescence emission. For the DMF/water mixtures, CN-NPFA intramolecular rotation is restricted due to space constraints, which suppresses the non-radiative decay of the excited state and enhances the fluorescent intensity. The solubility of CN-NPFA decreases and its concentration decreases, which leads to the reduction of fluorescence intensity after the moisture content exceeds 30%.

From a geometrical viewpoint, the α -cyanostilbene is of calamitic shape and can form a liquid crystalline phase after chemically endowing it with flexible tails. Prior to testing whether CN-NPFA is mesomorphic or not, a thermogravimetric analysis (TGA) measurement was conducted to evaluate its thermal

stability. As shown in Fig. S3, CN-NPFA is thermally very stable with an onset decomposition temperature as high as 308 °C. The mesomorphic properties of CN-NPFA were characterized using both differential scanning calorimetry (DSC) and polarized optical microscopy (POM). The phase-transition temperatures during first cooling and subsequent heating at a scan rate of 5 °C/min are depicted in the DSC curves – see Fig. 3(a). Four exothermic peaks were observed at 182 °C, 153 °C, 124 °C and 116 °C during the cooling process, whereas the endothermic peaks during the subsequent heating process were at 125 °C, 136 °C, 163 °C and 184 °C. Clearly, the highest transition temperature during cooling is rather close to that observed during heating, which indicates such transitions approach thermodynamic equilibrium, usually associated with liquid crystal transitions. The POM observations are in good agreement with the DSC results. Liquid crystalline phases were observed enantiotropically during both heating and cooling cycles. As shown in Fig. 3(b), a nematic liquid crystalline texture was observed using POM when it was cooled from its isotropic state to 175 °C. It can be identified by the Schlieren texture and indicates that CN-NPFA can behave as a liquid crystal. Moreover, after further

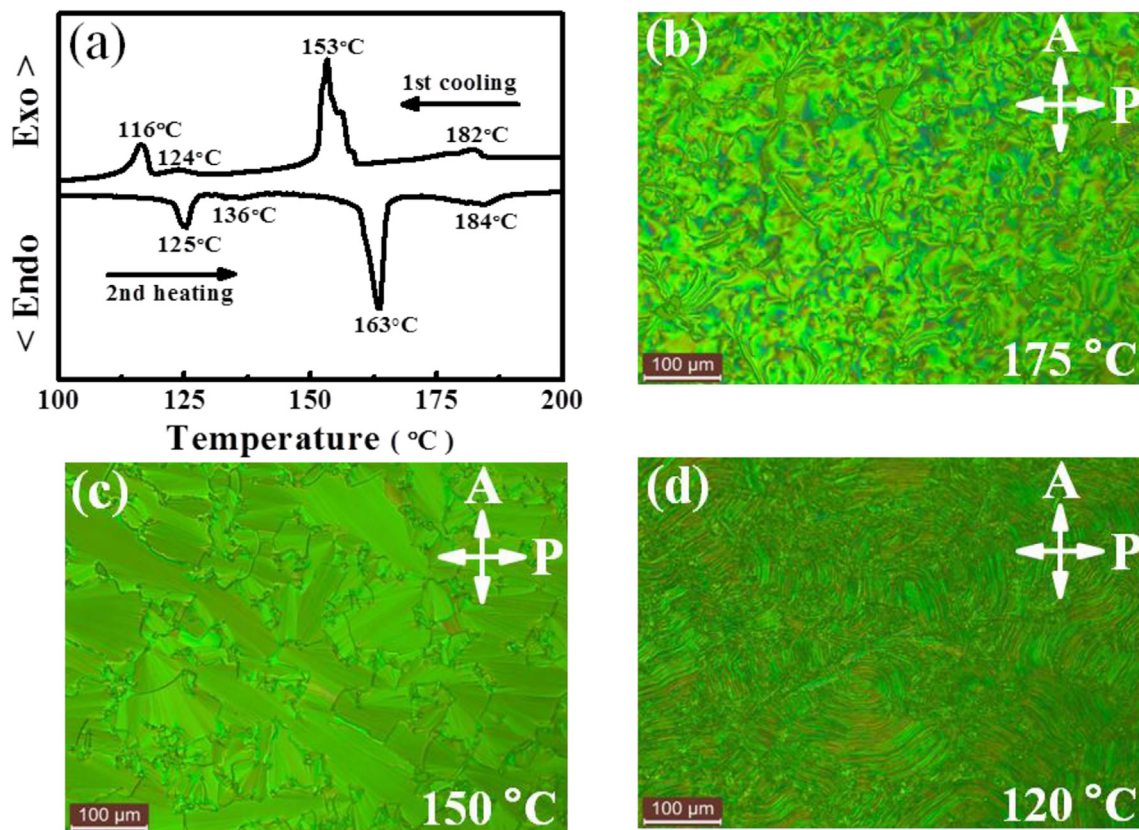


Fig. 3. (a) DSC curves of CN-NPFA at a heating/cooling rate of 5 °C per minute. (b–c) LC textures were recorded by POM at 175 °C, 150 °C, 120 °C as CN-NPFA first cooled from the isotropic melt.

cooling from the mesomorphic phase to 150 °C, a typical focal-conic fan-shaped texture of smectic C was formed – see Fig. 3(c). As the sample was cooled to a temperature lower than the third transition temperature, a smectic C* phase was observed – see Fig. 3(d). It can be identified by the striated fan-shaped texture. With the sample continuously cooled down to room temperature, crystallization of CN-NPFA occurred. When CN-NPFA was heated to its isotropic state, smectic C and nematic liquid crystal textures emerged, followed by smectic C* phase at 136 °C, 163 °C.

The alignment of the luminescent molecules plays a critical role in obtaining polarized fluorescent emission with a high dichroic ratio. Various methods have been developed to prepare the aligned luminescent layer, and some excellent reviews of preparation methods of aligned films are published. Mechanical friction is often used to prepare aligned films by rubbing the liquid crystal film with a cloth rod or by depositing the liquid crystal materials onto a rubbed aligned substrate, e.g. polyimide. In pursuit of highly polarized fluorescent emission, CN-NPFA molecules were first filled into 10 μm gap cells with antiparallel-rubbed polyimide alignment layers by capillarity action. The cell thickness was controlled with dispersion beads. Upon cooling to room temperature from the isotropic state with lower cooling rate (1 °C min⁻¹), an inhomogeneous optical texture of CN-NPFA was observed using POM – see Fig. S4(a). More precise observations were obtained using fluorescent microscopy (FM), by rotating the direction of the polarizer. During the FM analysis, we found the luminescence intensity does not vary significantly when the rubbing orientation was parallel or perpendicular to the polarizer – see Fig. S4(b). In order to study the luminescence anisotropy of the CN-NPFA films, we measured the polarized luminescence spectra, by rotating the direction of the

polarizer. Both the contrast ratio (R) and the degree of linear polarization (ρ) were determined from the spectra using Equations (1) and (2), respectively.

$$R = I_{\parallel} / I_{\perp} \quad (1)$$

$$\rho = (I_{\parallel} - I_{\perp}) / (I_{\parallel} + I_{\perp}) \quad (2)$$

Here I_{\parallel} and I_{\perp} represent the luminescent intensities when the polarizer-axes are parallel and perpendicular to the rubbing orientation, respectively. A contrast ratio of $R = 1.36$ was obtained for the CN-NPFA molecules in the rubbing cell, which indicates a lower linear polarization degree ($\rho = 0.15$). It is difficult to induce a smectic C* phase into an ordered arrangement via rubbing alignment. In addition, there is a significant angle (approximately 27°) between the emission dipole moment and the long molecular axis of the CN-NPFA molecule according to the DFT calculations – see Fig. S5. These produce the lower dichroism of the CN-NPFA film.

In order to obtain a single domain of the smectic C* phase, an electric field was applied using in-plane electrodes. A patterned ITO substrate was prepared with in-plane striped electrodes of 10 μm width and 10 μm spacing – see Fig. S6. When the CN-NPFA was cooled down to 174 °C from its isotropic state, a voltage of 200 V was applied, and a vague outline of LLC stripes was formed – see Fig. S7(a). The LLC domains are clearly aligned with the electrodes when the temperature dropped to 147 °C, which can be seen in Fig. S7(b). After the temperature decreased to 119 °C, the orientation of the LLC molecules becomes more ordered and the stripes gradually more homogeneous – see Fig. S7(c). Under the electric field, the LLC molecules rotate to form an ordered arrangement

where the polarization direction of the CN-NPFA molecules coincides with the electric field direction.

To confirm this molecular orientation, we analyze the POM of the aligned CN-NPFA films. As shown in Fig. S8, a distinct alternation of bright and dark fields was observed in the POM, when the films were rotated between the crossed polarizers. This indicates that the liquid crystal molecules were oriented uniaxially. Under an electric field, CN-NPFA molecules with a smectic layering structure rotate the title cone to form a ferroelectric structure due to dielectric polarization. As expected from this, the polar axis of the liquid crystal molecules is uniaxially aligned and parallel to the in-plane field between the electrodes. The optical axis of the CN-NPFA film was tilted towards the electric field and the angle between the electric field and the optical axis was approximately 30°. This is consistent with the angle between the dipole moment and the long molecular axis of the CN-NPFA molecule.

To demonstrate the versatility of our method, the luminescence from the aligned CN-NPFA films was investigated. As shown in the FM images in Fig. 4(a), a linearly polarized luminescent signal is observed with strong polarization-angle dependence. Relatively bright blue light appears when the electric field is parallel to the polarizer axis, showing a high fluorescent quantum yield ($\phi_f = 0.32$). Many studies have been conducted of the development of polarized luminescent illumination, which often required pre-patterned templates and complex processing steps. In this study, linearly polarized illumination could be generated from luminescent liquid crystals films, easily.

A further investigation of the orientation of the CN-NPFA molecules was carried out using polarized luminescence spectra. The aligned CN-NPFA film shows luminescent emission with a maximum wavelength at 458 nm when excited with light at a wavelength of 365 nm. The luminescence intensity from the aligned CN-NPFA molecules decreases as the azimuthal angle between the applied electric field and the polarizer changes from 0 to 90° – see Fig. 4(b). This enables sensitive probing of the molecular

orientation. According to calculations, the resulting ρ (0.71) indicates that the light is highly polarized. This is comparable to other linear polarized illumination systems like the electroluminescent system and fluorescent dye-doped system. In general, the molecular orientation affects the degree of linear polarization. Additionally, the order parameter (S) of the liquid crystalline directors can be determined using the following equation:

$$S = \frac{(I_{\parallel} - I_{\perp})}{(I_{\parallel} + 2I_{\perp})} = \frac{(R - 1)}{(R + 2)} \quad (3)$$

In our case, the value of S is 0.63, which is slightly higher than for the nematic LC phase. This means that the smectic-based illuminator can be used in a linear polarized illumination systems.

The surface profile of the aligned CN-NPFA film was investigated using confocal microscopy and a step profiler. As shown in Fig. 5(a) and (b), the LLC stripes shape of approximately 15 μm height were observed due to the dielectrophoretic effect. When CN-NPFA molecules are subjected to a non-uniform electric field, the CN-NPFA molecules are pulled toward the region where the gradient of the electric field is the highest. According to the simulation results shown in Fig. 5(c), when a voltage is applied across the ITO electrodes, the electric field is strongest near the edges of the ITO stripes. The largest gradient electric field and dielectric force would point toward this region. Thus, the CN-NPFA molecule prefers filling this region and two LLC lines are formed at the edges of the ITO stripe – see Fig. S9(b). Then, CN-NPFA in the two regions can grow up quickly and combine together due to the surface tension – see Figs. S9(c) and (d). This surface profile of the stripes was confirmed using a scanning electron microscope (Fig. S10).

To further improve the linear polarization, a rubbing alignment layer was prepared on the patterned ITO substrate. The angle between the rubbing direction and the electric field was about 27°. Table 1 shows the contrast ratio, the degree of linear polarization and the order parameter of CN-NPFA for different orientation methods. The results show a better aligned LLC film with a high

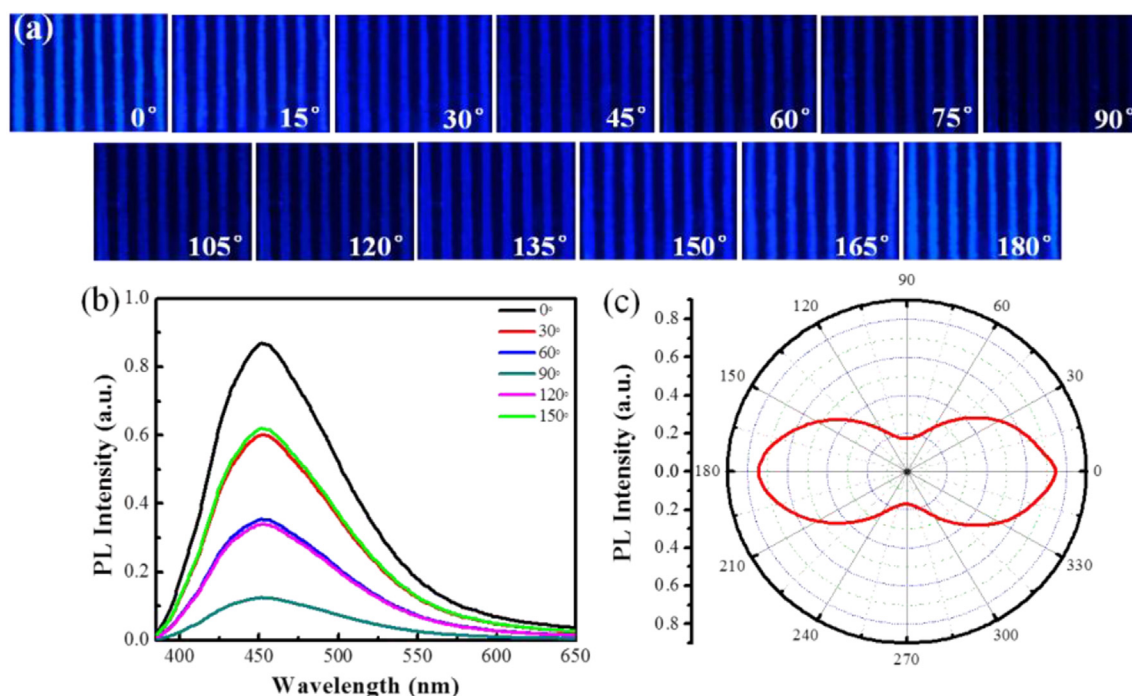


Fig. 4. (a) Photos of the luminescence for the field-induced uniaxial orientation of CN-NPFA film. The subtitles indicate the angle between the electric field and the orientation of the polarizer. (b) PL intensity as a function of wavelength for different polarizer axes. (c) The PL intensity profile with different polarizer axes for a wavelength of 458 nm.

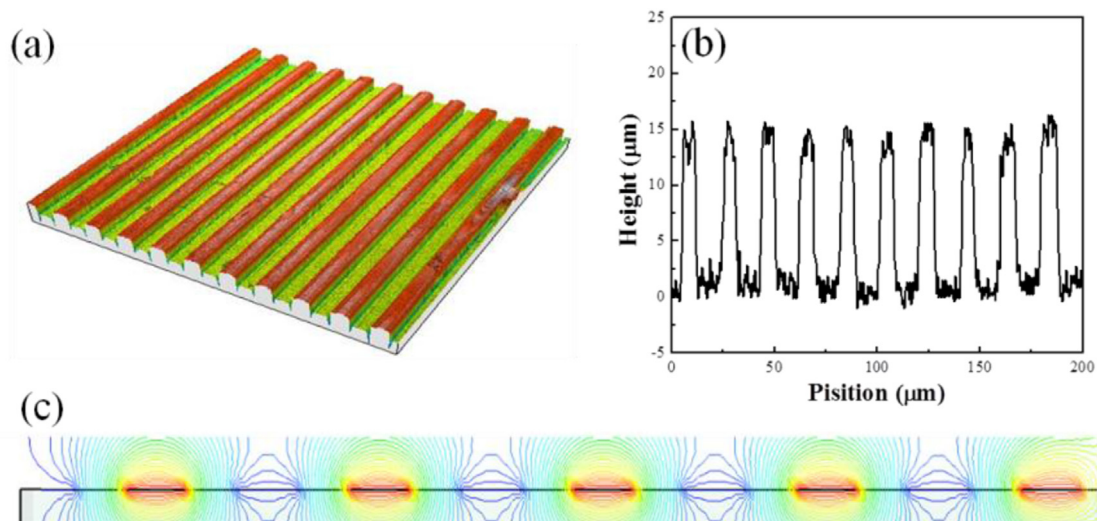


Fig. 5. (a) Surface morphology of the aligned CN-NPFA film detect using confocal microscopy. (b) Profile characterization of the aligned CN-NPFA film recorded on a step height measuring instrument. (c) Simulated electric-field distribution using the three-dimensional electromagnetic field simulation software CST.

Table 1

Contrast ratio, degree of linear polarization and order parameter of CN-NPFA for different orientation methods.

Method	Contrast ratio	degree of linear polarization	Order parameter
Rubbing alignment	1.36	0.15	0.11
Electric field induced alignment	6.16	0.71	0.63
Electric field induced alignment with a rubbing alignment layer	7.08	0.74	0.67

fluorescence quantum yield ($\phi_f = 0.36$) under the electric field with a rubbing alignment layer – see Fig. S11. LLC molecules can rotate to form an ordered arrangement, where the polarization direction of the CN-NPFA molecules follows the electric field direction and the long molecular axis of the CN-NPFA molecule follows the rubbing direction.

4. Conclusion

A novel AIEE-active LLC (CN-NPFA) was prepared, which shows three LC phases and a high fluorescence quantum yield. The in-plane electric field accompanying a rubbing alignment layer was used to obtain well-aligned CN-NPFA molecules domains over a large area, showing linearly polarized emission. The field-induced LLC film has regular stripe pattern with a high fluorescence quantum yield. The combination of AIEE with the described orientation technique of in-plane electrodes may advance LLC applications and prove helpful to future devices producing polarized luminescence.

Acknowledgements

The authors acknowledge the financial support of the National Natural Science Foundation of China (grant No. 61107014, 51573036), and Program for New Century Excellent Talents in University (Grant No. NCET-12-0839).

Appendix A. Supplementary data

Supplementary data related to this article can be found at <http://dx.doi.org/10.1016/j.orgel.2017.07.044>.

References

- [1] G. Martin, D.C.B. Donal, Polarized luminescence from oriented molecular materials, *Adv. Mater.* 11 (1999) 895.
- [2] H.B. Lu, S.J. Wu, C. Zhang, L.Z. Qiu, X.H. Wang, G.B. Zhang, J.T. Hu, J.X. Yang, Photoluminescence intensity and polarization modulation of a light emitting liquid crystal via reversible isomerization of an α -cyanostilbenic derivate, *Dyes Pigments* 128 (2016) 289.
- [3] G.G. Yury, A.K. Andrey, I.D. Vagif, C. Thomas, D. Kris, G.W. Christiane, B. Koen, Polarized luminescence from aligned samples of nematogenic lanthanide complexes, *Adv. Mater.* 20 (2008) 252.
- [4] Q. Ye, D.D. Zhu, H.X. Zhang, X.M. Lu, Q.H. Lu, Thermally tunable circular dichroism and circularly polarized luminescence of tetraphenylethene with two cholesterol pendants, *J. Mater. Chem. C* 3 (2015) 6997.
- [5] T.D. Nguten, E. Ehrenfreund, Z.V. Vardeny, The spin-polarized organic light emitting diode, *Synth. Met* 173 (2013) 16.
- [6] A. Liedtke, M.O. Neill, A. Wertmüller, S.P. Kitney, S.M. Kelly, White-light OLEDs using liquid crystal polymer networks, *Chem. Mater.* 20 (2008) 3579.
- [7] Y.T. Tsai, C.Y. Chen, L.Y. Chen, S.H. Liu, C.C. Wu, Y. Chi, S.H. Chen, H.F. Hsu, J.J. Lee, Analyzing nanostructures in mesogenic host-guest systems for polarized phosphorescence, *Org. Electron* 15 (2014) 311.
- [8] S.H. Liu, M.S. Lin, L.Y. Chen, Y.H. Hong, C.H. Tsai, C.C. Wu, A. Polоек, Y. Chi, C.A. Chen, S.H. Chen, H.F. Hsu, Polarized phosphorescent organic light-emitting devices adopting mesogenic host-guest systems, *Org. Electron* 12 (2011) 15.
- [9] J.H. Kim, A. Watanabe, J.W. Chung, Y. Jung, B.K. An, H. Tada, S.Y. Park, All-organic coaxial nanocables with interfacial charge-transfer layers: electrical conductivity and light-emitting-transistor behavior, *J. Mater. Chem.* 20 (2010) 1062.
- [10] M. Moriyama, N. Mizoshita, T. Yokota, K. Kishimoto, T. Kato, Photoresponsive anisotropic soft solids: liquid-crystalline physical gels based on a chiral photochromic gelator, *Adv. Mater.* 15 (2003) 1335.
- [11] T. Geelhaar, K. Griesar, B. Reckmann, 125 years of liquid crystals – a scientific revolution in the home, *Angew. Chem. Int. Ed.* 52 (2013) 8798.
- [12] M.J. Gim, S. Turlapati, S. Debnath, N.V. Rao, D.K. Yoon, Highly polarized fluorescent illumination using liquid crystal phase, *ACS. Appl. Mater. Interfaces* 8 (2016) 3143.
- [13] M.J. Gim, D.K. Yoon, Orientation control of smectic liquid crystals via a combination method of topographic patterning and in-plane electric field application for a linearly polarized illuminator, *ACS. Appl. Mater. Interfaces* 8 (2016) 27942.
- [14] E. Fleischmann, R. Zentel, ChemInform abstract: liquid crystalline ordering as a concept in materials science: from semiconductors to stimuli-responsive devices, *Angew. Chem. Int. Ed.* 52 (2013) 8810.
- [15] Y.F. Wang, J.W. Shi, J.H. Chen, W.G. Zhu, E. Baranoff, Recent progress in luminescent liquid crystal materials: design, properties and application for linearly polarized emission, *J. Mater. Chem. C* 3 (2015) 7993.
- [16] F. Camerel, J. Barberà, J. Otsuki, T. Tokimoto, Y. Shimazaki, L.Y. Chen, S.H. Liu, M.S. Lin, C.C. Wu, R. Ziessel, Solution-processable liquid crystals of luminescent aluminum (8-hydroxyquinoline-5-sulfonato) complexes, *Adv. Mater.* 20 (2008) 3462.
- [17] M.O. Neill, S.M. Kelly, Liquid crystals for charge transport, luminescence, and photonics, *Adv. Mater.* 15 (2003) 1135.
- [18] H.T. Wang, F.L. Zhang, B.L. Bai, P. Zhang, J.H. Shi, D.Y. Yu, Y.F. Zhao, Y. Wang,

- M. Li, Synthesis, liquid crystalline properties and fluorescence of polycatenar 1,3,4-oxadiazole derivatives, *Liq. Cryst.* 35 (2008) 905.
- [19] A.C. Sentman, D.L. Gin, Fluorescent trimeric liquid crystals: modular design of emissive mesogens, *Adv. Mater.* 13 (2001) 1398.
- [20] V.D. Halleux, J.P. Calbert, P. Brocorens, J. Cornil, J.P. Declercq, J.L. Brédas, Y. Geerts, 1,3,6,8-Tetraphenylpyrene derivatives: towards fluorescent liquid-crystalline columns? *Adv. Funct. Mater.* 14 (2004) 649.
- [21] C.H. Ting, J.T. Chen, C.S. Hsu, Synthesis and thermal and photoluminescence properties of liquid crystalline polyacetylenes containing 4-alkoxyphenyl trans-4-alkylcyclohexanoate side groups, *Macromolecules* 35 (2002) 1180.
- [22] W.Z. Yuan, Z.Q. Yu, P. Lu, C.M. Deng, J.W. Lam, Z.M. Wang, E.Q. Chen, Y.G. Ma, B.T. Tang, High efficiency luminescent liquid crystal: aggregation-induced emission strategy and biaxially oriented mesomorphic structure, *J. Mater. Chem.* 22 (2012) 3323.
- [23] W.B. Jia, H.W. Wang, L.M. Yang, H.B. Lu, L. Kong, Y.P. Tian, X.T. Tao, J.X. Yang, Synthesis of two novel indolo[3,2-b]carbazole derivatives with aggregation-enhanced emission property, *J. Mater. Chem. C* 1 (2013) 7092.
- [24] X. Du, Z.Y. Wang, Donor-acceptor type silole compounds with aggregation-induced deep-red emission enhancement: synthesis and application for significant intensification of near-infrared photoluminescence, *Chem. Commun.* 47 (2011) 4276.
- [25] J.W. Chung, S.J. Yoon, B.K. An, S.Y. Park, High-contrast on/off fluorescence switching via reversible EeZ isomerization of diphenylstilbene containing the α -cyanostilbenic moiety, *J. Phys. Chem. C* 117 (2013) 11285.
- [26] H.B. Lu, S.N. Zhang, A.X. Ding, M. Yuan, G.Y. Zhang, W. Xu, G.B. Zhang, X.H. Wang, L.Z. Qiu, J.X. Yang, A luminescent liquid crystal with multistimuli tunable emission colors based on different molecular packing structures, *New. J. Chem.* 38 (2014) 3429.
- [27] H.B. Lu, S.J. Wu, J.L. Hu, L.Z. Qiu, X.H. Wang, G.B. Zhang, J.T. Hu, G.Q. Lv, J.X. Yang, Electrically controllable fluorescence of tristable optical switch based on luminescent molecule-doped cholesteric liquid crystal, *Dyes Pigments* 121 (2015) 147.